AFRL-RZ-WP-TR-2011-2057

MULTISPECTROSCOPIC (FTIR, XPS, AND TOFMS-TPD) INVESTIGATION OF THE CORE-SHELL BONDING IN SONOCHEMICALLY-PREPARED ALUMINUM NANOPARTICLES CAPPED WITH OLEIC ACID (PREPRINT)

Andrew T. Rosenberger, Donald K. Phelps, Jonathon E. Spowart, and Christopher E. Bunker

Fuels and Energy Branch
Energy/Power/Thermal Division

William K. Lewis, Christopher A. Crouse, Barbara A. Harruff, K. A. Shiral Fernando, Marcus J. Smith, and Elena A. Guliants

University of Dayton Research Institute

APRIL 2010

AIR FORCE RESEARCH LABORATORY
PROPULSION DIRECTORATE
WRIGHT-PATTERSON AIR FORCE BASE, OH 45433-7251
AIR FORCE MATERIEL COMMAND
UNITED STATES AIR FORCE

NOTICE AND SIGNATURE PAGE

This report was cleared for public release by the USAF 88th Air Base Wing (88 ABW) Public Affairs (AFRL/PA) Office and is available to the general public, including foreign nationals. Copies may be obtained from the Defense Technical Information Center (DTIC) (http://www.dtic.mil).

AFRL-RZ-WP-TP-2011-2057 HAS BEEN REVIEWED AND IS APPROVED FOR PUBLICATION IN ACCORDANCE WITH THE ASSIGNED DISTRIBUTION STATEMENT.

*//Signature//
CHRISTOPHER E. BUNKER
Project Engineer
Fuels and Energy Branch
Energy/Power/Thermal Division

//Signature//
MIGUEL A. MALDONADO, Acting Chief
Fuels and Energy Branch
Energy/Power/Thermal Division
Propulsion Directorate

REPORT DOCUMENTATION PAGE

Form Approved
OMB No. 0704-0188

1. REPORT DATE *(DD-MM-YY)*	2. REPORT TYPE	3. DATES COVERED *(From - To)*
April 2010	Journal Article Preprint	01 May 2009 – 01 December 2009

4. TITLE AND SUBTITLE

MULTISPECTROSCOPIC (FTIR, XPS, AND TOFMS-TPD) INVESTIGATION OF THE CORE-SHELL BONDING IN SONOCHEMICALLY-PREPARED ALUMINUM NANOPARTICLES CAPPED WITH OLEIC ACID (PREPRINT)

5a. CONTRACT NUMBER
In-House

5b. GRANT NUMBER

5c. PROGRAM ELEMENT NUMBER
62203F

6. AUTHOR(S)

Andrew T. Rosenberger, Donald K. Phelps, Jonathon E. Spowart,
and Christopher E. Bunker (AFRL/RZPF)
William K. Lewis, Christopher A. Crouse, Barbara A. Harruff, K.A. Shiral Fernando,
Marcus J. Smith, and Elena A. Guliants (University of Dayton Research Institute)

5d. PROJECT NUMBER
5330

5e. TASK NUMBER
5B

5f. WORK UNIT NUMBER
5330SBF1

7. PERFORMING ORGANIZATION NAME(S) AND ADDRESS(ES)

Fuels and Energy Branch (AFRL/RZPF)
Energy/Power/Thermal Division
Air Force Research Laboratory, Propulsion Directorate
Wright-Patterson Air Force Base, OH 45433-7251
Air Force Materiel Command, United States Air Force

University of Dayton Research Institute
300 College Park
Dayton, OH 45469-0110

8. PERFORMING ORGANIZATION REPORT NUMBER
AFRL-RZ-WP-TP-2011-2057

9. SPONSORING/MONITORING AGENCY NAME(S) AND ADDRESS(ES)

Air Force Research Laboratory
Propulsion Directorate
Wright-Patterson Air Force Base, OH 45433-7251
Air Force Materiel Command
United States Air Force

10. SPONSORING/MONITORING AGENCY ACRONYM(S)
AFRL/RZPF

11. SPONSORING/MONITORING AGENCY REPORT NUMBER(S)
AFRL-RZ-WP-TP-2011-2057

12. DISTRIBUTION/AVAILABILITY STATEMENT
Approved for public release; distribution unlimited.

13. SUPPLEMENTARY NOTES
Report contains color. PA Case Number: 88ABW-2009-5257; Clearance Date: 21 Dec 2009.
Journal article submitted to the *J. Phys. Chem. C.*

14. ABSTRACT

Organically-capped metal nanoparticles are an attractive alternative to more conventional oxide-passivated materials, due to the lower reaction temperatures and the possibility of tuning the organic coating. Sonochemical methods have been used to produce air-stable aluminum nanoparticles capped with oleic acid. In order to understand the nature of the metal-organic bonding in this system, we have used FTIR, XPS, and TOFMS-TPD techniques to study the organic passivation layer and its desorption at elevated temperatures. In the present case we find that the organic layer appears to be attached via Al-O-C bonds with the C atom formerly involved in the carboxylic acid functional group.

15. SUBJECT TERMS

16. SECURITY CLASSIFICATION OF:			17. LIMITATION OF ABSTRACT:	18. NUMBER OF PAGES	19a. NAME OF RESPONSIBLE PERSON (Monitor)
a. REPORT	b. ABSTRACT	c. THIS PAGE			Christopher E. Bunker
Unclassified	Unclassified	Unclassified	SAR	22	19b. TELEPHONE NUMBER *(Include Area Code)* N/A

Table of Contents

List of Figures

1.0 SUMMARY

Organically-capped metal nanoparticles are an attractive alternative to more conventional oxide-passivated materials, due to the lower reaction temperatures and the possibility of tuning the organic coating. Sonochemical methods have been used to produce air-stable aluminum nanoparticles capped with oleic acid. In order to understand the nature of the metal-organic bonding in this system, we have used FTIR, XPS, and TOFMS-TPD techniques to study the organic passivation layer and its desorption at elevated temperatures. In the present case we find that the organic layer appears to be attached via Al-O-C bonds with the C atom formerly involved in the carboxylic acid functional group.

2.0 INTRODUCTION

Aluminum particles and their oxidation mechanisms have become a focus of ongoing interest due to the high heat of reaction associated with formation of aluminum oxide, namely 31 kJ/g aluminum burned[1]. Of course, in order to efficiently harness the stored chemical energy of aluminum particles, it is desirable for the particles to oxidize completely. Nanoparticles are advantageous in this regard, since they tend to oxidize more fully and more quickly than micron-scale and larger particles. In addition to the size of the particle, the passivation method also plays a key role in determining the reactivity.

Typically, aluminum particles are passivated by a naturally occurring oxide shell several nanometers thick that spontaneously forms upon exposure to air. This oxide shell is quite effective at protecting the particle from further reaction, and elevated temperatures of 500-600 ^{o}C are required to trigger oxidation of the remaining aluminum metal[2-4]. However, many potential energetic applications for aluminum nanoparticles would benefit from a lower reaction onset temperature, particularly if the onset temperature is tunable. An additional difficulty posed by the conventional oxide shell as that the fraction of the particle consumed by the oxide becomes large for nanoparticles. Because the oxide shell itself is unreactive towards further oxidation, the energy content for these smaller particles is decreased.

As a result of these factors, it is desirable to develop alternative methods of passivation such a capping the aluminum particle with an organic layer[5-7]. Organically-capped aluminum nanoparticles have been produced via sonochemical methods that are air-stable at ambient temperatures, but at elevated temperatures (~150-400 ^{o}C) reaction begins with thermal loss and combustion of the organic shell[7]. Following removal of the organic layer, the exposed aluminum core can then be oxidized. A particularly attractive possibility would be to tune the reaction onset temperature of the nanoparticles by varying the choice of capping agent.

Clearly it is important to understand the nature of the bonding between the organic protecting layer and the metallic core in such particles in order to control and predict the reactivity. In the current study, we have synthesized small (< 10 nm average size) aluminum nanoparticles capped with oleic acid, and used Fourier Transform Infrared (FTIR), X-Ray Photoelectron Spectroscopy (XPS) and Temperature Programmed Desorption (TPD) to characterize the interaction between the metallic and organic components of the particles.

3.0 METHODS, ASSUMPTIONS, AND PROCEDURES

3.1 Materials

Alane N,N-dimethylethylamine in a 0.4 M toluene solution, titanium (IV) isopropoxide (98%), oleic acid (99%), dodecane (99% and anhydrous), and oleyl alcohol (99%) were all obtained from Aldrich and used as received. Hexane (Optima grade) was obtained from Fisher Scientific. Nanometer-scale aluminum oxide was obtained from Nanocomposites, Inc.

3.2 Synthesis of Aluminum Nanoparticles

The procedures used to synthesize oleic acid-capped aluminum nanoparticles have been described in detail elsewhere[7]. Briefly, aluminum nanoparticles were synthesized using an initial solution of 11.4 mM oleic acid dissolved in dodecane. The solution was subjected to several freeze-pump-thaw cycles in order to reduce the dissolved oxygen concentration and then placed inside a dry nitrogen glovebox, where alane N,N-dimethylethylamine and a titanium (IV) isopropoxide catalyst were added to the solution. The concentrations of the alane complex and titanium catalyst in this solution were 50 and 0.55 mM, respectively. This solution was then transferred into a sonication flask (Sonics Inc., Suslick flask) and sonicated. The sonication instrument (Sonics Inc. Vibra Cell) was operated at 20 kHz, and sonicated the solution at 37% power (~22W) for 7.5 min active time, using a 1-s-on, 1-s-off duty cycle. During sonication, the bulk solution temperature reached approximately 70 ^{o}C. These conditions produced a black solution that gradually precipitated a grayish-black powder. The powder was recovered by evaporation of the solvent under vacuum, followed by repeated washings with hexane. The aluminum nanoparticles produced by this process were spherical, with an average size of ~5 nm and a size distribution of 2-15 nm.

Organically coated aluminum oxide particles were synthesized via a refluxing procedure. A 10.5 mg sample of the nano-aluminum oxide was heated to ~120 ^{o}C for several mintues to drive off any adsorbed water. These particles were placed in a flask and 8 mL of dodecane and 18 μL of oleic acid were added. The mixture was then refluxed at 130 ^{o}C for 24 hours. A white powder was recovered by evaporation of the solvent under vacuum, followed by repeated washings with hexane.

3.3 Characterization of Aluminum Nanoparticles

Infrared absorption spectra of the nanoparticles were collected using a Perkin-Elmer L100 FTIR equipped with an attenuated total reflectance (ATR) sample attachment. X-ray photoelectron spectroscopy (XPS) was performed on a Surface Science Instruments M-Probe using monochromatic Al K_{α} x-rays (energy 1486.6 eV). Samples were prepared by casting a drop of particles suspended in hexanes onto a 10 mm x 10 mm silicon wafer coated with a native oxide and allowing the solvent to evaporate, leaving behind a thin film. Time-of-flight mass spectrometry / temperature programmed desorption (TOFMS-TPD) measurements were performed using a linear time-of-flight mass spectrometer (Jordan TOF Products, Inc.) equipped with a temperature-controlled sample stage with line-of-sight into the ionization region. The temperature ramp rate was 10 ^{o}C /min. Ionization of the vapor effusing from the heated nanoparticle sample was provided by an electron impact source at 70 eV incident energy.

4.0 RESULTS AND DISCUSSION

Our characterization of the metal-organic bonding in oleic acid-capped nanoparticles begins with FTIR spectroscopy. In Figure 1 we show the IR spectra of neat oleic acid, oleic acid-capped aluminum oxide nanoparticles, and oleic acid capped aluminum nanoparticles. In the spectrum of oleic acid (Fig. 1a), the most prominent features are the C-H stretching peaks between 2800-3000 cm^{-1} and the carbonyl stretch at ~1700 cm^{-1}. A broad OH feature is also visible under the C-H stretching signals. Additionally, there are several signals in the "fingerprint region" below 1400 cm^{-1} corresponding to various low frequency modes of the molecule.

In the spectrum of the oleic acid-capped aluminum oxide nanoparticles (Fig. 1b), we see that the C-H stretches are largely unaffected, but that the carbonyl stretching peak is no longer observed and two prominent peaks at ~1465 and ~1585 cm^{-1} have appeared. These peaks are characteristic of symmetric and asymmetric carboxylate (COO) stretches, indicating that oleic acid is chemisorbed to the surface via its oxygen atoms. It has been shown from a survey of carboxylic acids bonded to metal surfaces that the frequency difference between the symmetric and asymmetric modes can be used to assign the bonding geometry[8-10]. The observed splitting of ~120 cm^{-1} most likely indicates a bridging, or possibly bidentate, bonding geometry in the case of Al_2O_3-oleic acid. We also note that a strong O-H feature is observed from 3000-3600 cm^{-1}, probably resulting from hydrogen (liberated during formation of the carboxylate species) binding to the aluminum oxide in order to form surface OH groups. The large absorption below 1000 cm^{-1} corresponds an aluminum oxide bulk absorption[11-13].

The FTIR absorption spectrum of the aluminum-oleic acid nanoparticles is shown in Figure 1c. We again find that the C-H stretches are unchanged from those found in the spectrum of oleic acid, and that the carbonyl peak has disappeared. Additionally, we observe a broad OH band visible from ~3000-3700 cm^{-1}. In this spectrum, however, we do not observe the strong symmetric and asymmetric carboxylate stretching bands seen in the Al_2O_3-oleic acid case above. There are some weaker bands between 1300-1600 cm^{-1}, and it is tempting to assign them to a carboxylate as well, but we must be cautious in our interpretation here, since other IR active modes such as C-H and O-H bending modes can be found in this region of the spectrum.

At first glance, these data would seem to be consistent with earlier surface science investigations into the bonding of carboxylic acids to aluminum and aluminum oxide surfaces. These have shown that carboxylic acids react with aluminum oxide to form carboxylates on the surface[8-10]. These carboxylates are quite stable, and can be heated to temperatures of ~500 ^{o}C before they begin to desorb[14]. For carboxylic acids binding to aluminum metal, the situation is more complex; the nature of the bonding observed changes with temperature. At low temperature (120 K), carboxylic acids deprotonate and bind to the surface via the two oxygen atoms in the acid group, again forming a carboxylate[8-10]. However, due to the high reactivity of aluminum, as the surface is warmed to room temperature the carboxylates begin to decompose[8,10,14-17]. X-ray photoelectron spectroscopy (XPS) measurements have shown that during decomposition of the carboxylate, the two oxygen atoms are stripped away to form oxide islands[15], and a structure is formed in which the remaining alkyl chain binds directly to the surface through an Al-C bond formed from the carbon atom associated with the decomposed functional group[14,15]. At room temperature, both intact carboxylates and the decomposed structures involving Al-C bonds can be observed but at elevated temperatures, only the latter

remain[14]. At yet higher temperatures (T > 200 ^{o}C), the alkyl chain begins to decompose as well[14].

These processes are consistent with the chief features of the IR spectra, namely that the oleic acid-capped Al_2O_3 nanoparticles would exhibit C-H stretching signals from the alkyl chain as well as intense carboxylate bands corresponding to the reacted functional group. On the other hand, oleic acid-capped Al nanoparticles would show only the C-H stretches, owing to the decomposition of the carboxylate that then results in attachment of the alkyl chain via an Al-C bond. In this is the case, the XPS spectrum of these nanoparticles should feature a prominent Al-C peak, as was the case in the earlier surface science studies.

In Figure 2, we show XPS spectra of the Al-oleic acid nanoparticles in the O1s, C1s, and Al2p regions. In the O1s region (Fig. 2a), we find a strong signal between 530-534 eV, where Al_xO_y and Al-O-C signals have been observed previously[14,15]. In the C1s vicinity (Fig. 2b) we find a peak centered at ~285.5 eV, assigned to aliphatic carbon, and a small shoulder at ~289.5 eV, which may be due to intact carboxylates[14]. In the Al2p spectrum in Figure 2c, we find a signal at ~75 eV from Al_xO_y and another at ~72.5 eV corresponding to Al metal[15]. But we find no Al-C signals in these spectra, which we would expect to appear between 282-283 eV in the C1s region[14,15]. This fact would seem to refute the idea that carboxylates have decomposed as described above, and suggests that some other type of binding is present in our system.

An important clue is providing by temperature-programmed desorption (TPD) data. The oleic acid-capped aluminum nanoparticles were heated at a rate of 10 ^{o}C /min from room temperature up to 600 ^{o}C and a mass spectrum was recorded at various temperatures using time-of-flight mass spectrometry (TOF-MS). The integrated signal in the mass spectrum as a function of temperature is shown in Figure 3 and indicates that the organic coating begins to desorb at ~300 ^{o}C. The small signals recorded at lower temperatures are simply due to residual solvents evaporating from the nanoparticle sample. Above 300 ^{o}C, the signals rapidly increase as the spectrum shown in Figure 4a grows in. Comparison of this spectrum with the standard mass spectrum databases[18] reveals the spectrum to be that of oleyl alcohol. The molecular ion is just visible at 268 amu, an H_2O elimination peak appears at 250 amu, and a series of additional fragments appear at lower masses. To confirm the assignment, a mass spectrum of oleyl alcohol was also recorded and is shown in Figure 4b. The two spectra are virtually identical with the exception of two peaks at 91 and 92 amu, respectively, in the spectrum of the oleyl alcohol sample. These are assigned to an impurity, since they do not appear in the literature spectrum of oleyl alcohol[18] and the integrated intensity of these peaks relative to the remainder of the spectrum is consistent with the manufacturer-stated purity of the sample.

These results give us new insight into the nature of the metal-organic binding, particularly when combined with the results from the FTIR and XPS experiments. We know from the IR spectrum of the oleic-acid capped aluminum nanoparticles that C-H and O-H groups are present, but that carbonyl signals are absent. We also observe little, if any, carboxylate signal. The XPS results confirm the presence of aliphatic carbon, and indicate the presence of Al-O and/or Al-O-C bonds, but show no Al-C bonds. Finally, TOFMS-TPD has shown that when the nanoparticles are heated, the organic coating desorbs as oleyl alcohol. These observations suggest a structure similar to that shown in Figure 5, which would seem to satisfy all of the above constraints. Indeed, infrared spectroscopy measurements on alkoxy-coated metal[19,20] and metal oxide[21,22] surfaces have shown that the most prominent features in the

spectrum are C-H stretching peaks at ~2800-3200 cm^{-1} and an O-C stretching band in the vicinity of 800-1000 cm^{-1}. The proposed structure would exhibit these signals as well as an O-H stretch, in agreement with our experimental spectrum.

Although TPD measurements on metal surfaces coated with this structure are not available, experiments with methoxy-coated aluminum surfaces[23] have shown that upon heating the O-C bonds break, leaving O atoms bonded to the aluminum metal and desorbing methane. Analogously, we might expect the structure in Figure 5 to desorb oleyl alcohol when heated, again consistent with the experimental results. We note that a hydrogen atom must be abstracted from another source in order for an approaching oleic acid molecule to form the surface structure in Figure 5, and again in order to produce oleyl alcohol following O-C bond rupture. The former is not too difficult to imagine given that the synthesis takes place in solution. The source of the hydrogen atom in the latter process is currently unclear, but most likely it is obtained from a neighboring molecule or an adsorbed impurity. Regardless of the mechanism, the same behavior was observed in the above study[23] of methoxy-coated surfaces as well.

The fact that the nature of metal-organic binding observed in the present case is somewhat different than that observed in previous surface science studies of carboxylic acids binding to aluminum and aluminum oxide surfaces is likely a consequence of the surface characteristics. For our nanoparticles, the surface is neither a well-ordered Al_2O_3 phase, nor a pristine Al metal surface. Our previous work has shown that the surface is only partially oxidized, and exhibits reactivity towards further oxidation once the organic coating is removed[7]. It is perhaps not surprising that the surface characteristics would affect the bonding scheme since surface science experiments on clean and oxidized copper surfaces have also found that the nature of the metal-organic interactions can vary significantly with the extant of surface oxidation[24].

Alternatively, the observed bonding motif may be the result of the high temperatures (5000 K) and rapid cooling (10^{10} K/s) processes present in the sonochemical environment[25], which have been shown to result in formation of non-equilibrium structures such as metallic glasses[26]. This explanation seems less likely, however, since we have previously shown that our aluminum particles are not formed by the traditional sonochemical processes of microbubble formation and collapse and as such are expected to experience more modest temperature gradients[7]. Nevertheless, the present results have allowed us to characterize the metal-organic bonding in detail and suggest that the nature of the bonding in our sonochemically-prepared aluminum nanoparticles is somewhat different than that typically associated with carboxylic acids interacting with metal and metal oxide surfaces.

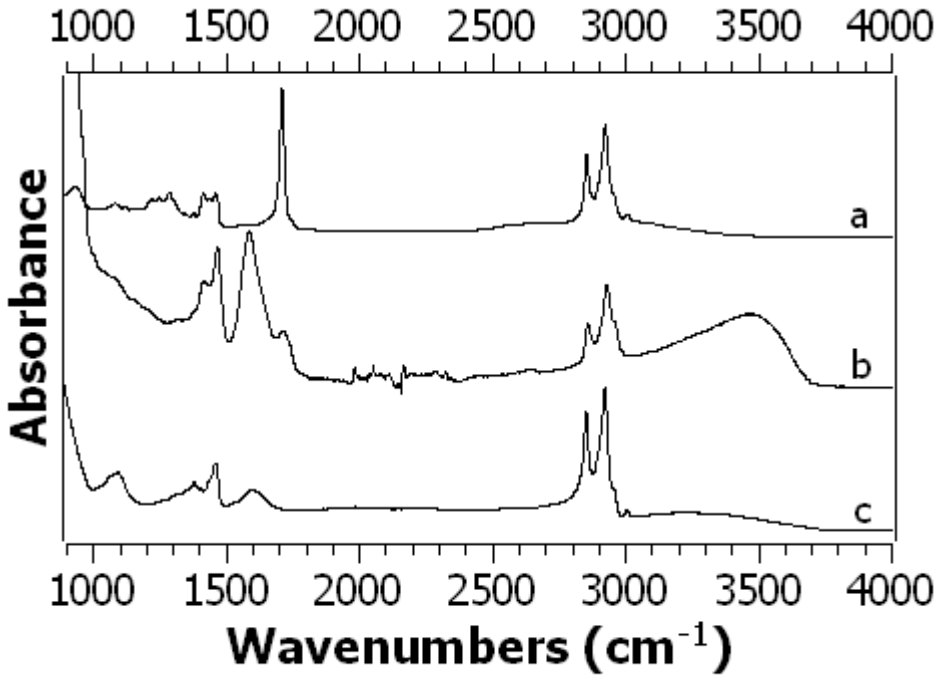

Figure 1

FTIR spectra of (a) neat oleic acid, (b) aluminum oxide nanoparticles coated with oleic acid, and (c) sonochemically-produced aluminum nanoparticles capped with oleic acid. Intense carboxylate stretches between ~1465 and ~1585 cm^{-1} are observed in the spectrum of the aluminum oxide particles, but these signals are absent in the aluminum-oleic acid case.

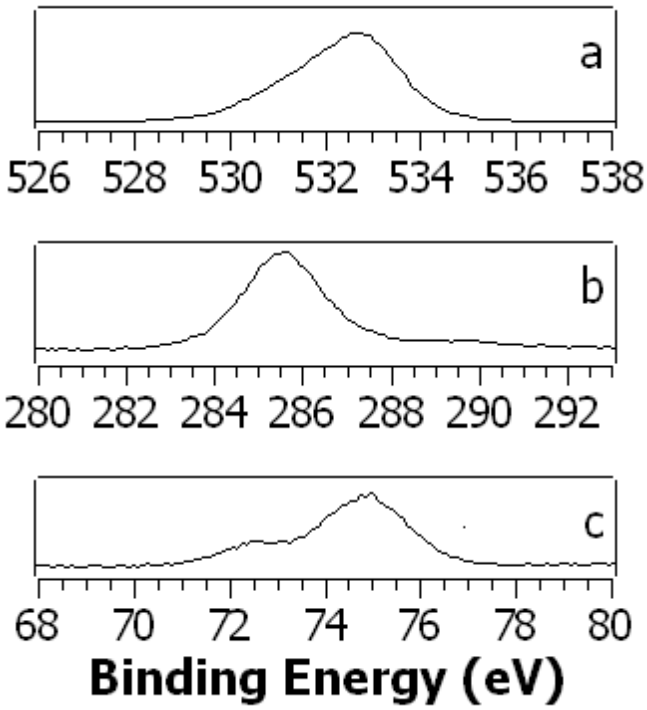

Figure 2

XPS spectra of the oleic acid-capped aluminum nanoparticles in the O1s (a), C1s (b), and Al2p (c) regions. We find a strong signal between 530-534 eV, where Al_xO_y and Al-O-C signals have been reported, but we find no evidence of Al-C bonds, which would expected to exhibit a peak between 282-283 eV[14,15].

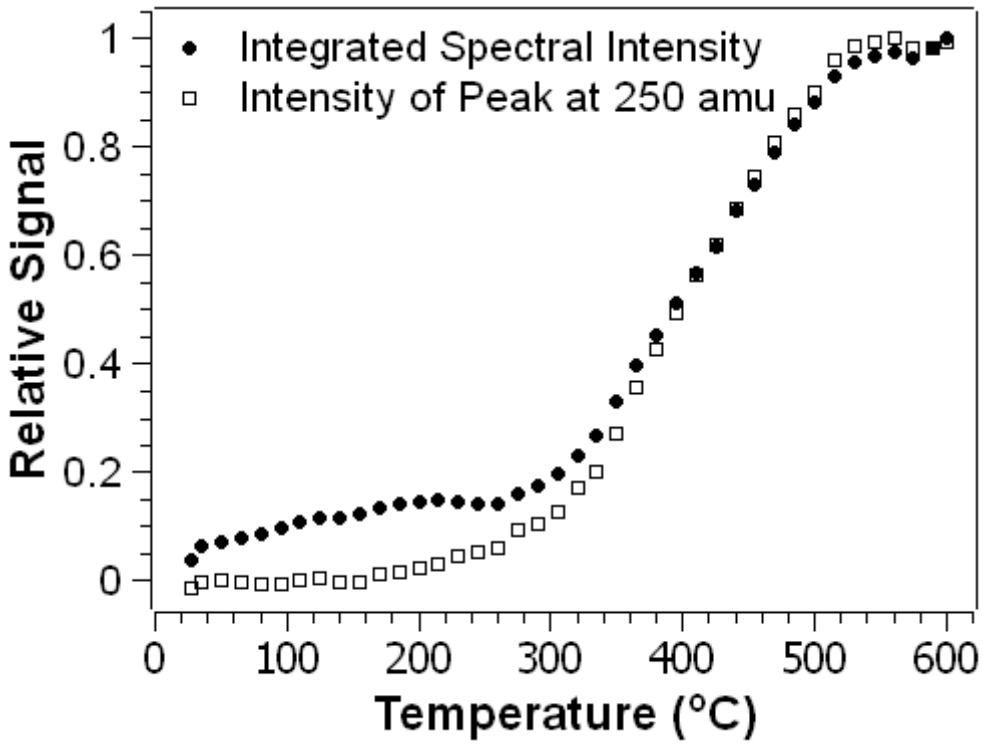

Figure 3

Temperature programmed desorption (TPD) trace showing the intensity of the signals contained in the time-of-flight mass spectrum as a function of the temperature. The temperature ramp rate was 10 ^{o}C /min. Below 300 ^{o}C, signal is generated by residual solvents evaporating from the sample. As the sample is heated above 300 ^{o}C, the solvent signals abate and the spectrum shown in Figure 4a grows in.

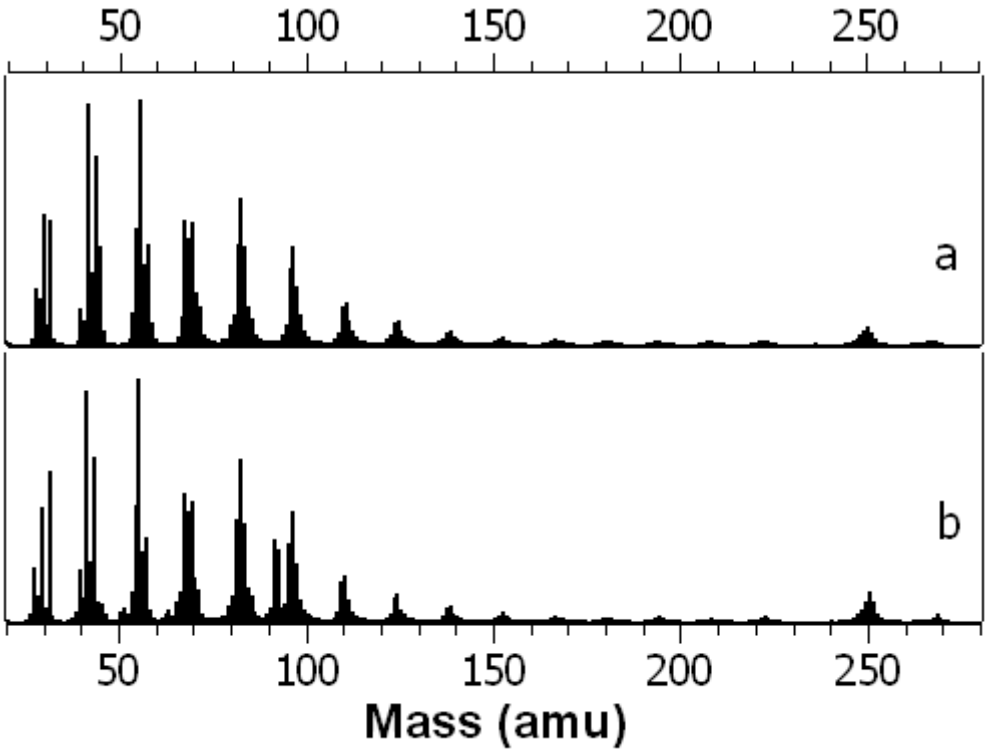

Figure 4

Mass spectrum of the vapor leaving the oleic acid-capped aluminum nanoparticle sample (a), collected at 560 ^{o}C. The spectrum matches that of oleyl alcohol found in the standard mass spectrum databases[18]. For comparison, the spectrum of an oleyl alcohol sample (99% purity) is also shown (b). The spectrum are nearly identical except for small impurity signals at 91 and 92 amu, respectively, in the latter.

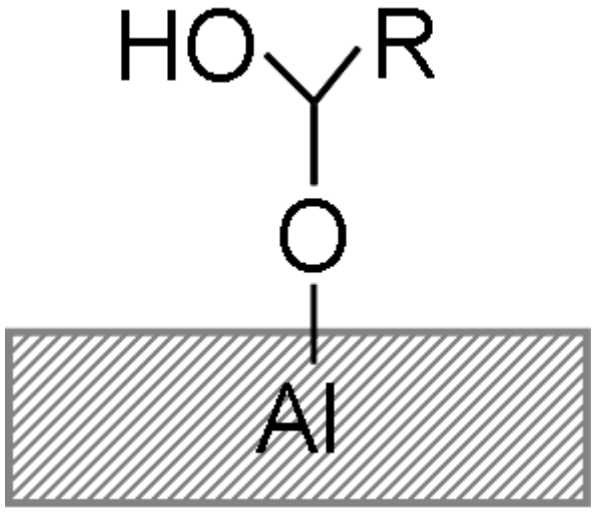

Figure 5
Proposed structure to explain the combined FTIR, XPS, and TOFMS-TPD observations. The group "R" represents the alkyl chain $(CH_2)_7CH=CH(CH_2)_7CH_3$.

5.0 CONCLUSION

We have used FTIR, XPS, and TOFMS-TPD methods to characterize the metal-organic bonding between aluminum and an oleic acid capping agent in sonochemically-prepared aluminum nanoparticles. In contrast to earlier surface science work on carboxylic acids attached to metal and metal oxide surfaces, in the present case we find that the capping agent is bound neither as a carboxylate nor via Al-C bonds resulting from decomposed carboxylates. Instead the organic layer appears to be attached via Al-O-C bonds with the C atom formerly involved in the carboxylic acid functional group.

6.0 ACKNOWLEDGMENT

We gratefully acknowledge financial support from the Defense Threat Reduction Agency (DTRA) under Grant no. HDTRA-07-1-0026, the Air Force Office of Scientific Research (AFOSR) through the continued support of Dr. Julian Tishkoff, and the Air Force Research Laboratory (AFRL) through the NanoEnergetics program.

7.0 REFERENCES

1. *CRC Handbook of Chemistry and Physics*, 80th edition, edited by D. R. Lide (CRC, Cleveland, 2000).

2. Trunov, M. A.; Schoenitz, M.; Zhu, X.; Dreizin, E. L. *Combust. Flame* **2005**, *140*, 310–318.

3. Sun, J.; Pantoya, M. L.; Simon, S. L. *Thermochim. Acta* **2006**, *444*, 117–127.

4. Morgan, A. B.; Wolf, J. D.; Guliants, E. A.; Fernando, K. A. S.; Lewis, W. K. *Thermochim. Acta* **2009**, *488*, 1-9.

5. Jouet, R. J.; Warren, A. D.; Rosenberg, D. M.; Bellitto, V. J.; Park, K.; Zachariah, M. R. *Chem. Mater*. **2005**, *17*, 2987–2996.

6. Jouet, R. J.; Granholm, R. H.; Sandusky, H. W.; Warren, A. D. In *Shock Compression of Condensed Matter-2005*; Proceedings of the Conference of the American Physical Society Topical Group on Shock Compression of Condensed Matter, Baltimore, MD, July 31-August 5, 2005; Furnish, M. D., Elert, M., Russell, T. P., White, C. T., Eds.; American Institute of Physics: 2006, 1527.

7. Fernando, K. A. S.; Smith, M. J.; Harruff, B. A.; Lewis, W. K.; Bunker, C. E. *J. Phys. Chem. C* **2009**, *113*, 500-503.

8. Crowell, J. E.; Chen, J. G.; Yates, J. T., Jr. *J. Chem. Phys*. **1986**, *85*, 3111.

9. Deacon, G. B.; Phillips, R. J. *Coord. Chem. Rev*. **1980**, *33*, 227.

10. Crowell, J. E.; Chen, J. G.; Yates, J. T., Jr. *J. Electron Spectrosc. Relat. Phenom.* **1986**, *39*, 97-106.

11. Erskine, J. L.; Strong, R. L. *Phys. Rev. B* **1982,** *25*, 5547.

12. Strong, R. L.; Firey, B.; deWette, F. W.; Erskine, J. L. *Phys. Rev. B* **1982,** *26*, 3483.

13. Crowell, J. E.; Chen, J. G.; Yates, J. T. *Surf. Sci.* **1986,** *165*, 37.

14. Underhill, R.; Timsit, R. S. *J. Vac. Sci. Technol. A* **1992**, *10*, 2767-2774.

15. Bournel, F.; Laffon, C.; Parent, Ph., Tourillon, G. *Surf. Sci.*, **1996**, *352-354*, 228-231.

16. Chen, J. G.; Crowell, J. E.; Yates, J. T. *Surf. Sci.* **1986**, *172*, 733-753.

17. Davies, P. R.; Roberts, M. W.; Shukla, N. *J. Phys. Condens. Matter* **1991**, *3*, S237-S244.

18. NIST Mass Spec Data Center, S. E. Stein, director. "Mass Spectra"; In *NIST Chemistry WebBook, NIST Standard Reference Database Number 69*; Linstrom, P. J., Mallard, W. G., Eds.; National Institute of Standards and Technology: Gaithersburg MD, 2009; http://webbook.nist.gov.

19. Andersson, M. P.; Uvdal, P.; MacKerell, A. D. Jr. *J. Phys. Chem. B* **2002**, *106*, 5200-5211.

20. Asmundsson, R.; Uvdal, P.; MacKerell, A. D. Jr *J. Chem. Phys.* **2000**, *113*, 1258-1267.

21. Camplin, J. P.; McCash, E. M. *Surf. Sci.* **1996**, *360*, 229-241.

22. Wu, W-C.; Chuang, C-C.; Lin, J-L. *J. Phys. Chem. B* **2000**, *104*, 8719-8724.

23. Sardar, S. A.; Syed, J. A.; Tanaka, K.; Netzer, F. P.; Ramsey, M. G. *Surf. Sci.* **2002**, *519*, 218-228.

24. Carley, A. F.; Davies, P. R.; Mariotti, G. G. *Surf. Sci.* **1998**, *401*, 400-411.

25. Suslick, K. S. *Science* **1990**, *247*, 1439-1445.

26. Suslick, K. S.; Choe, S-B.; Cichowlas, A. A.; Grinstaff, M. W. *Nature* **1991**, *353*, 414-416.

LIST OF ACRONYMS AND ABBREVIATIONS

AFOSR	Air Force Office of Scientific Research
AFRL	Air Force Research Laboratory
Al	aluminum
Al_2O_3	aluminum oxide
Al_xO_y	alumina
Al2p	aluminum energy transition
Al-C	aluminum-carbon bond
Al-O	aluminum-oxygen bond
Al-O-C	aluminum-oxygen-carbon bond/chain
ATR	Attenuated Total Reflectance
amu	atomic mass units
C	carbon
C1s	carbon energy transition
C-H	carbon-hydrogen bond
cm	centimeter
cm^{-1}	wavenumber
COO	carboxylate
DTRA	Defense Threat Reduction Agency
eV	electron volts
FTIR	Fourier Transform Infrared
g	gram
H	hydrogen
H_2O	water
IR	infrared
K	Kelvin
K/s	Kelvins per second

kHz	kilohertz
kJ	kilojoule
K_{α}	describes the type of X-Ray source
M	molar
mg	milligram
min	minute
mL	milliliter
mM	millimolar
mm	millimeter
N	nitrogen
nm	nanometer
O	oxygen
O1s	oxygen energy transition
OH	hydroxyl
O-H	oxygen-hydrogen bond
s	second
T	temperature
TOF-MS	Time-of-Flight Mass Spectrometry
TOFMS-TPD	Time of Flight Mass Spectrometry/Temperature Programmed Desorption
TPD	Temperature Programmed Desorption
USA	United States of America
W	watt
XPS	X-Ray Photoelectron Spectroscopy
°C	degrees Celsius
°C/min	degrees Celsius per minute
µL	micro liter